Cell Reports

Supplemental Information

Direct Involvement of Retinoblastoma Family Proteins in DNA Repair by Non-homologous End Joining

Rebecca Cook, Georgia Zoumpoulidou, Maciej T. Luczynski, Simone Rieger, Jayne Moquet, Victoria J. Spanswick, John A. Hartley, Kai Rothkamm, Paul H. Huang, and Sibylle Mittnacht

Figure S1

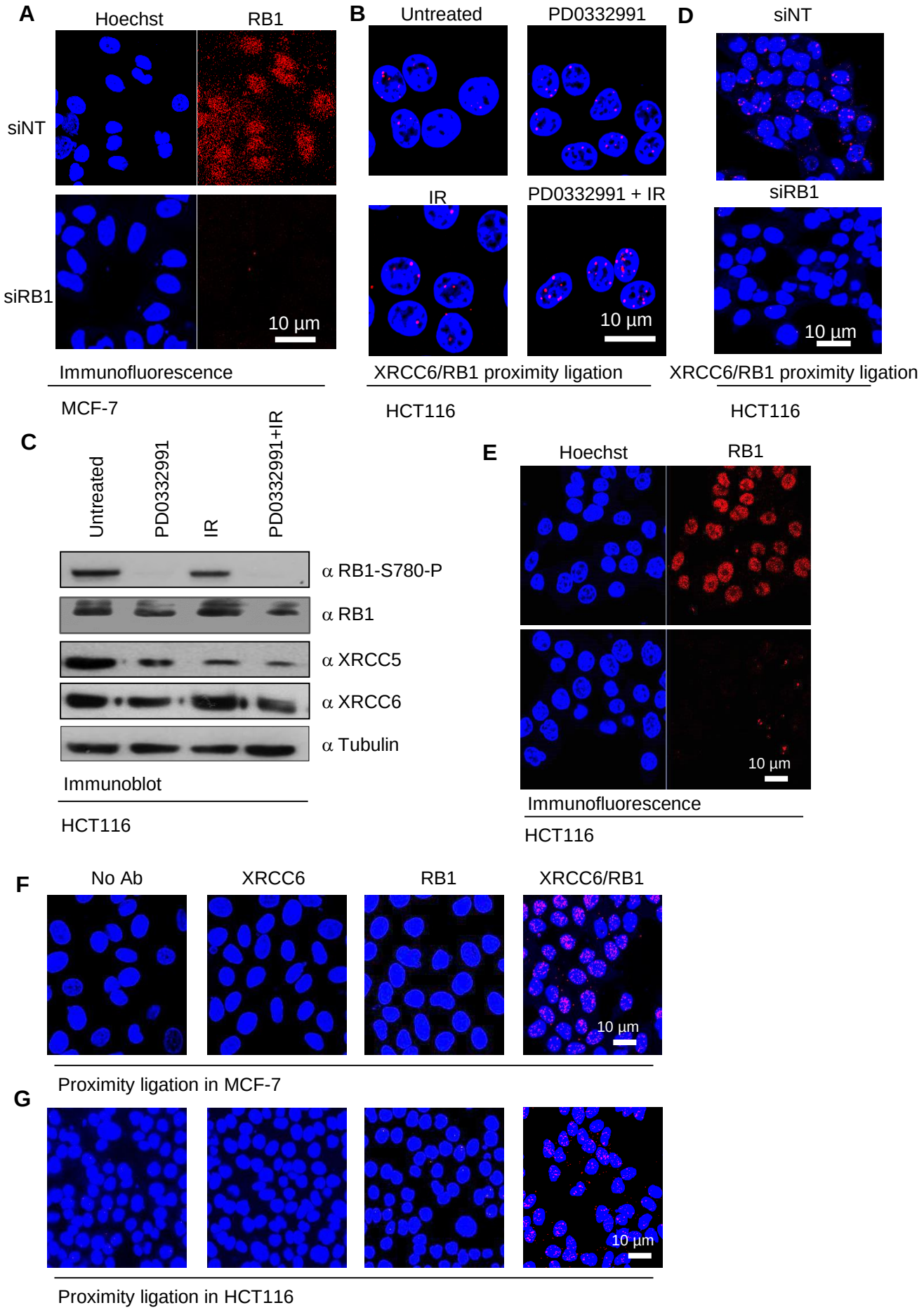
A
Hoechst
RB1
siNT
siRB1
10 µm
Immunofluorescence
MCF-7
B
Untreated
PD0332991
IR
PD0332991 + IR
10 µm
XRCC6/RB1 proximity ligation
HCT116
D
siNT
siRB1
10 µm
XRCC6/RB1 proximity ligation
HCT116
C
Untreated
PD0332991
IR
PD0332991+IR
α RB1-S780-P
α RB1
α XRCC5
α XRCC6
α Tubulin
Immunoblot
HCT116
E
Hoechst
RB1
10 µm
Immunofluorescence
HCT116
F
No Ab
XRCC6
RB1
XRCC6/RB1
10 µm
Proximity ligation in MCF-7
G
10 µm
Proximity ligation in HCT116

Figure S2

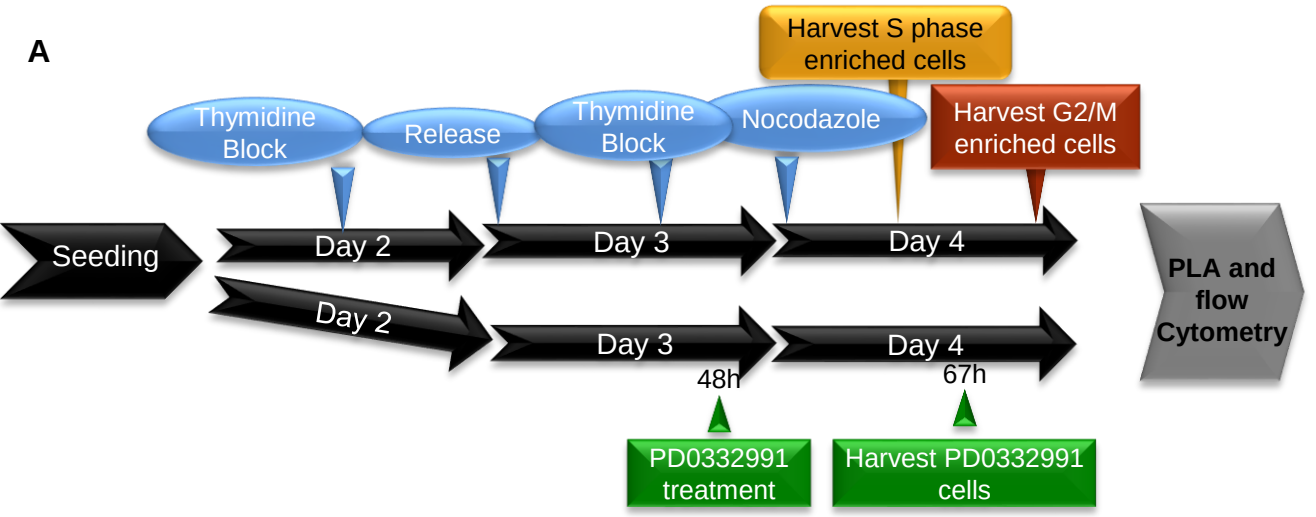
A
Harvest S phase enriched cells
Thymidine Block
Release
Thymidine Block
Nocodazole
Harvest G2/M enriched cells
Seeding
Day 2
Day 3
Day 4
PLA and flow Cytometry
Day 2
Day 3
Day 4
48h
67h
PD0332991 treatment
Harvest PD0332991 cells

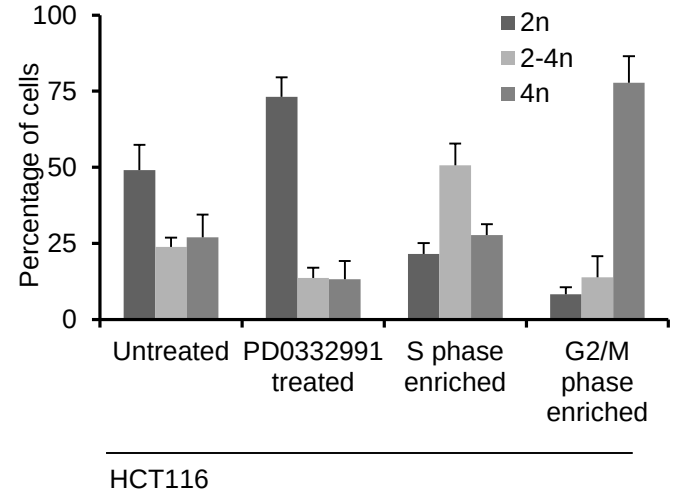
B
100
75
50
25
0
Percentage of cells
2n
2-4n
4n
Untreated
PD0332991 treated
S phase enriched
G2/M phase enriched
HCT116

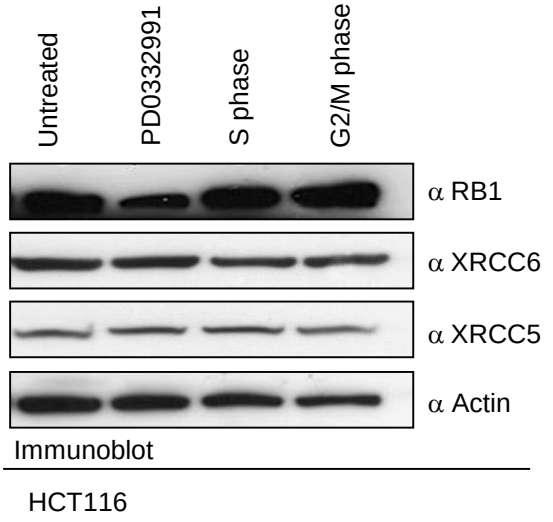
C
Untreated
PD0332991
S phase
G2/M phase
α RB1
α XRCC6
α XRCC5
α Actin
Immunoblot
HCT116

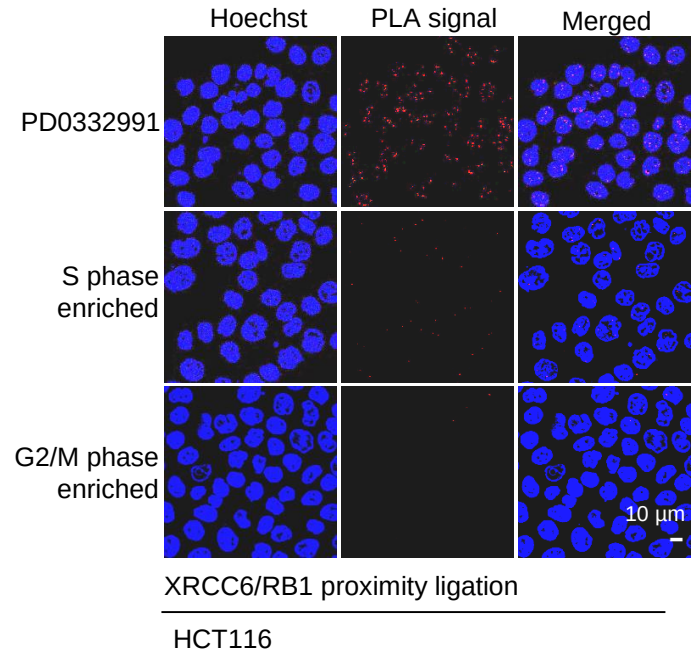
D
Hoechst
PLA signal
Merged
PD0332991
S phase enriched
G2/M phase enriched
10 µm
XRCC6/RB1 proximity ligation
HCT116

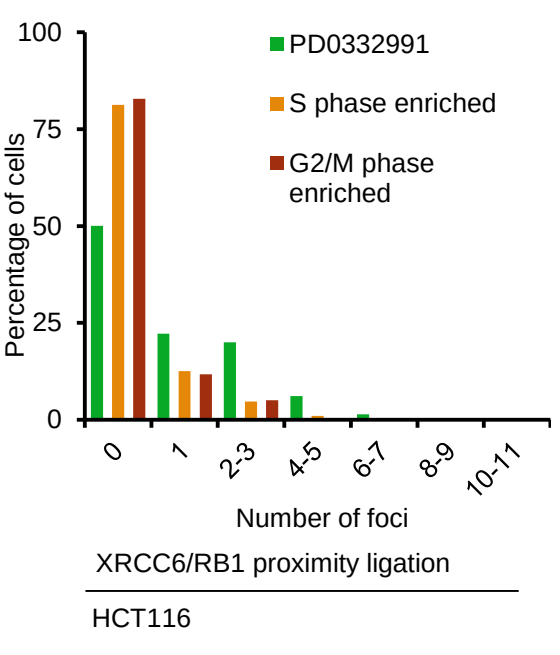
E
100
75
50
25
0
Percentage of cells
PD0332991
S phase enriched
G2/M phase enriched
0
1
2-3
4-5
6-7
8-9
10-11
Number of foci
XRCC6/RB1 proximity ligation
HCT116

A

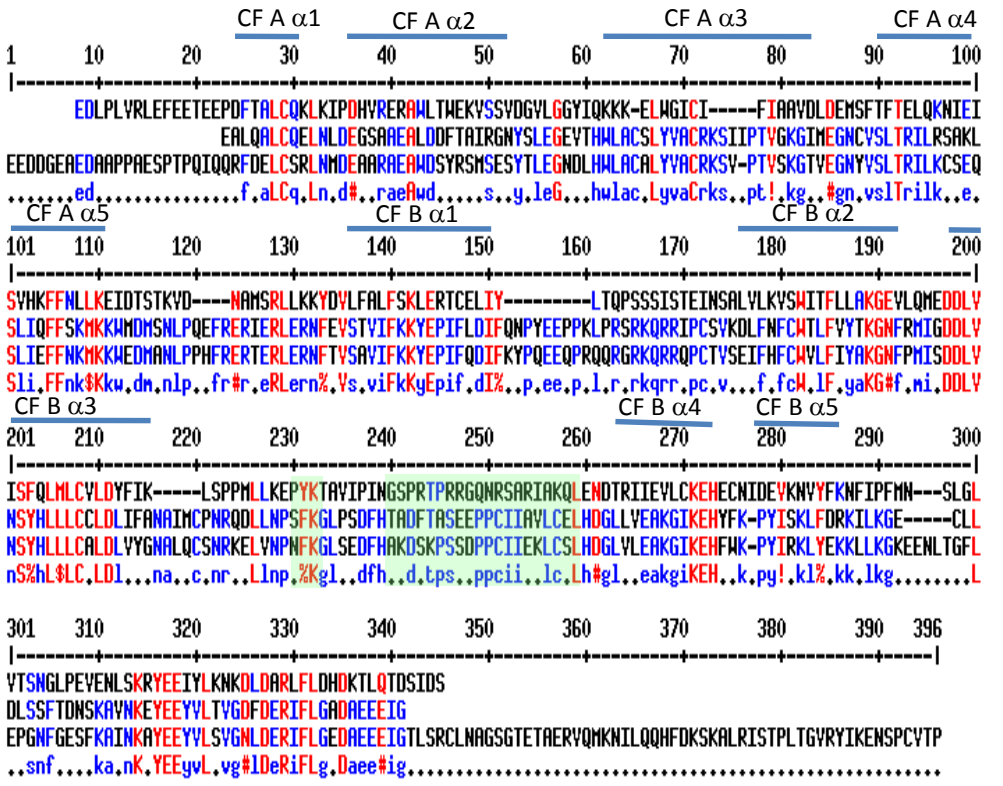
RB1N aa40-355
RBL1N aa19-330
RBL2N aa24-418
consensus
CF A α1
CF A α2
CF A α3
CF A α4
CF A α5
CF B α1
CF B α2
CF B α3
CF B α4
CF B α5

B

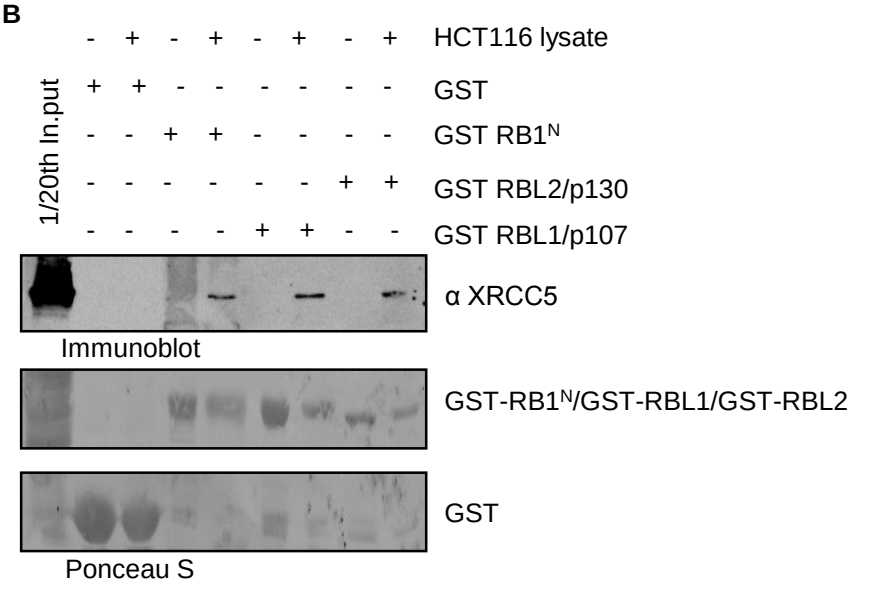
1/20th Input
HCT116 lysate
GST
GST RB1N
GST RBL2/p130
GST RBL1/p107
α XRCC5
Immunoblot
GST-RB1N/GST-RBL1/GST-RBL2
GST
Ponceau S

Figure S4

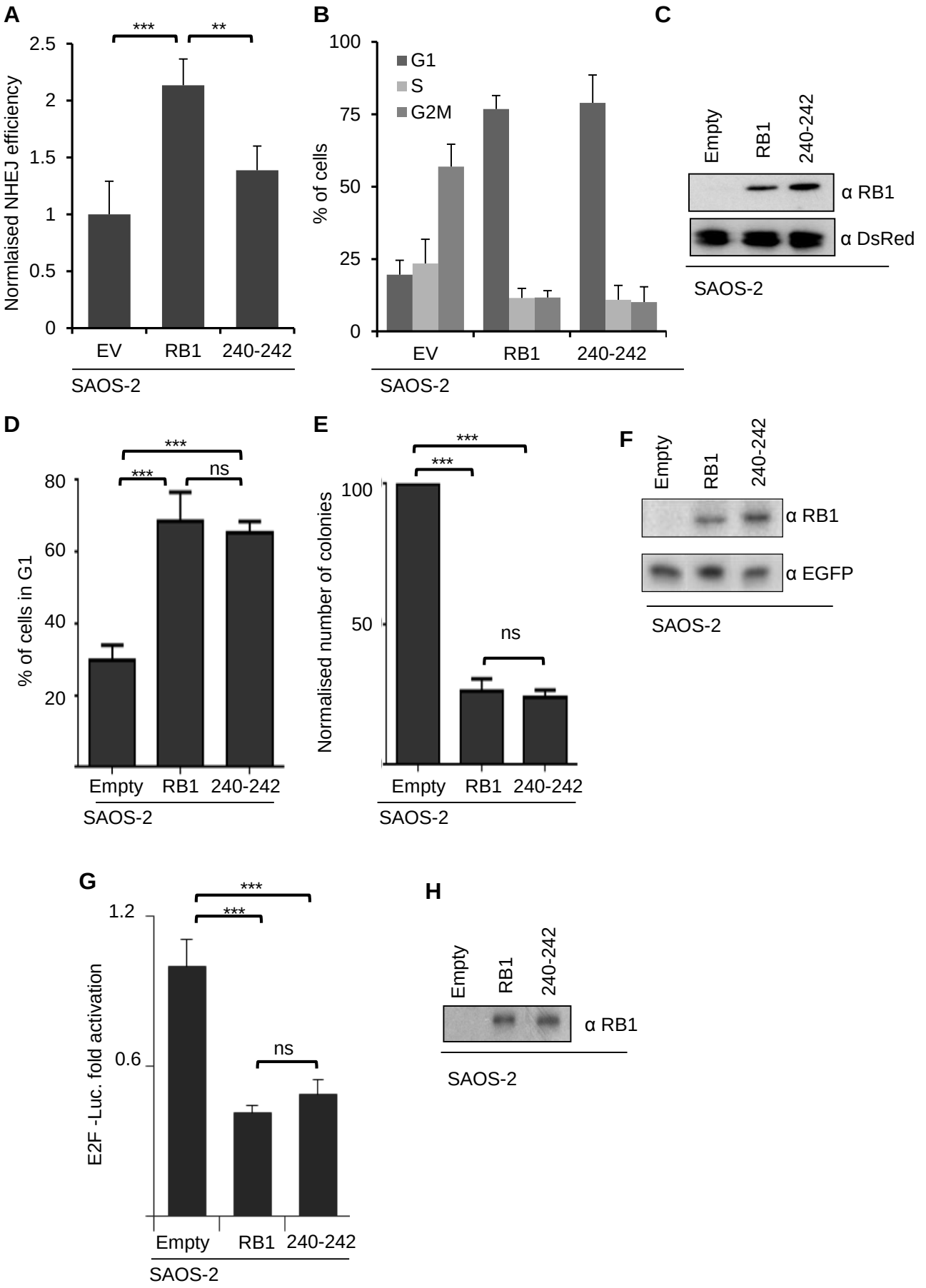
A
***
**
2.5
2
1.5
1
0.5
0
Normlaised NHEJ efficiency
EV
RB1
240-242
SAOS-2
B
100
75
50
25
0
% of cells
G1
S
G2M
EV
RB1
240-242
SAOS-2
C
Empty
RB1
240-242
α RB1
α DsRed
SAOS-2
D
***
***
ns
80
60
40
20
% of cells in G1
Empty
RB1
240-242
SAOS-2
E
***
***
100
50
Normalised number of colonies
ns
Empty
RB1
240-242
SAOS-2
F
Empty
RB1
240-242
α RB1
α EGFP
SAOS-2
G
***
***
1.2
0.6
E2F -Luc. fold activation
ns
Empty
RB1
240-242
SAOS-2
H
Empty
RB1
240-242
α RB1
SAOS-2

Figure S5

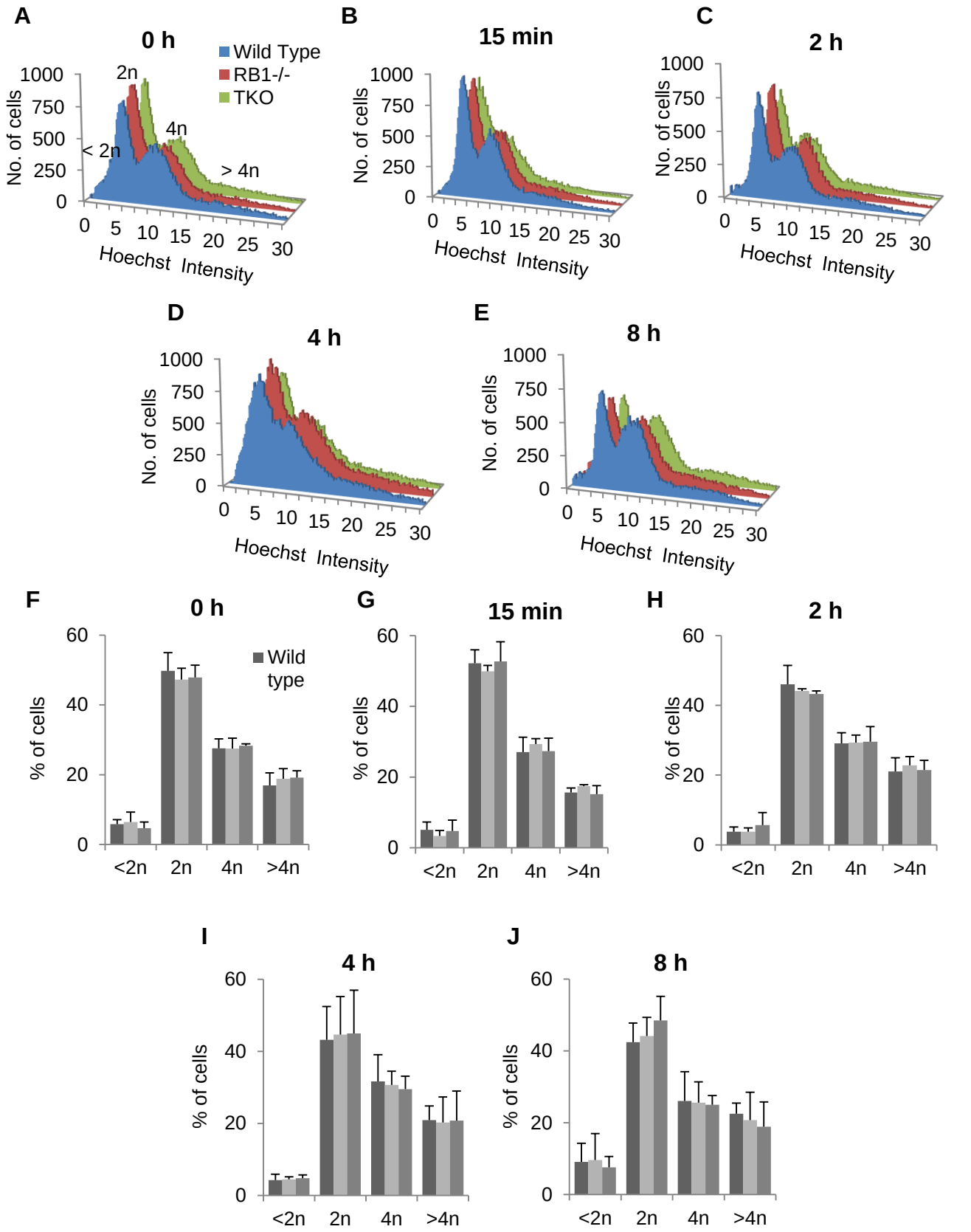
A
0 h
Wild Type
RB1-/-
TKO
2n
4n
< 2n
> 4n
No. of cells
1000
750
500
250
0
0 5 10 15 20 25 30
Hoechst Intensity
B
15 min
C
2 h
D
4 h
E
8 h
F
0 h
Wild type
% of cells
60
40
20
0
<2n 2n 4n >4n
G
15 min
H
2 h
I
4 h
J
8 h

A

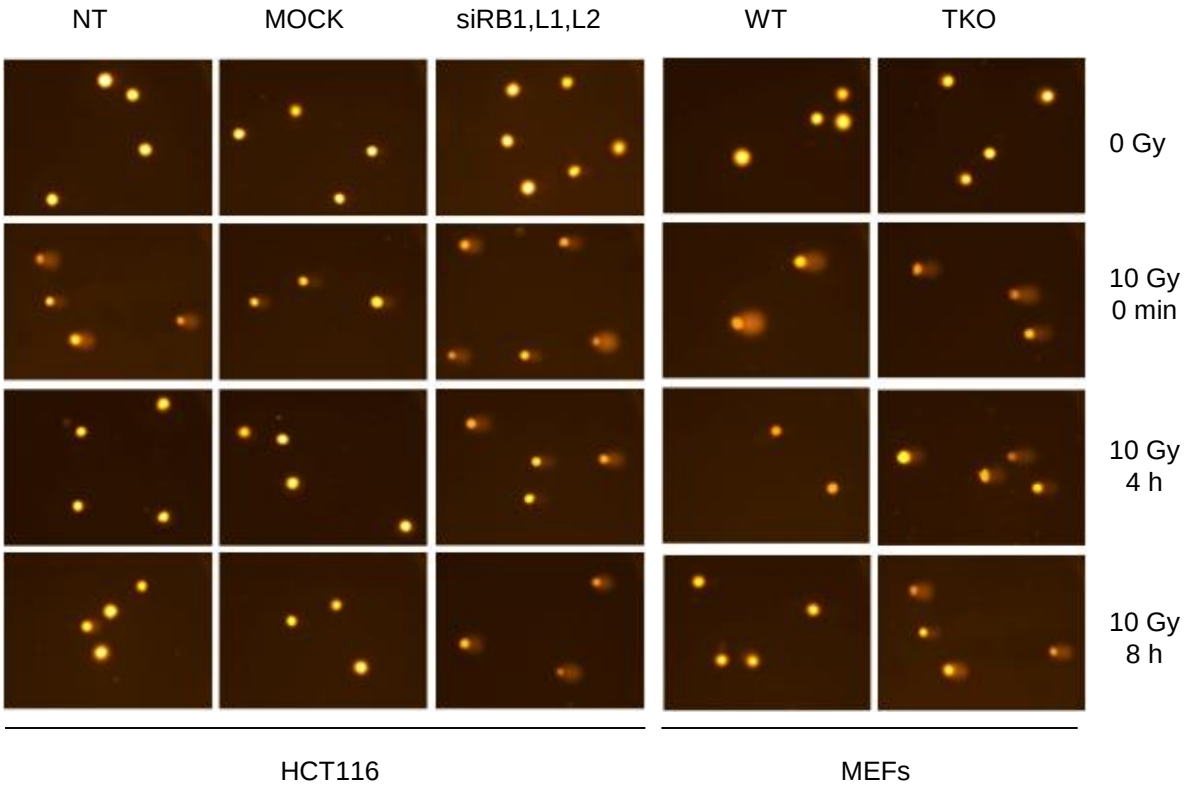
NT
MOCK
siRB1,L1,L2
WT
TKO
0 Gy
10 Gy
0 min
10 Gy
4 h
10 Gy
8 h
HCT116
MEFs

B

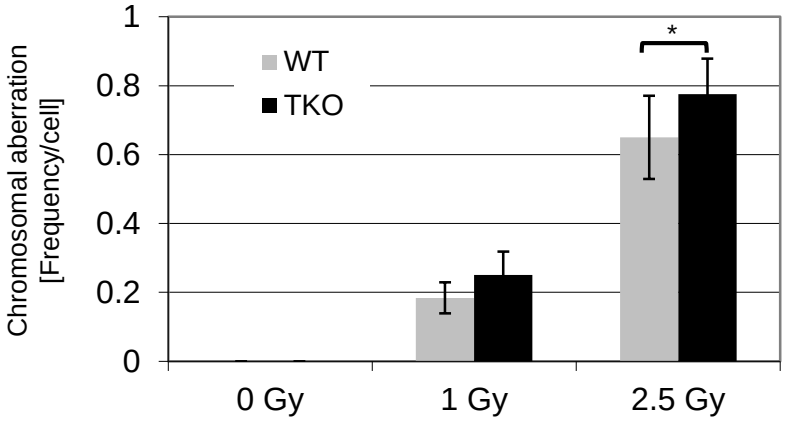
Chromosomal aberration
[Frequency/cell]
1
0.8
0.6
0.4
0.2
0
WT
TKO
*
0 Gy
1 Gy
2.5 Gy

C

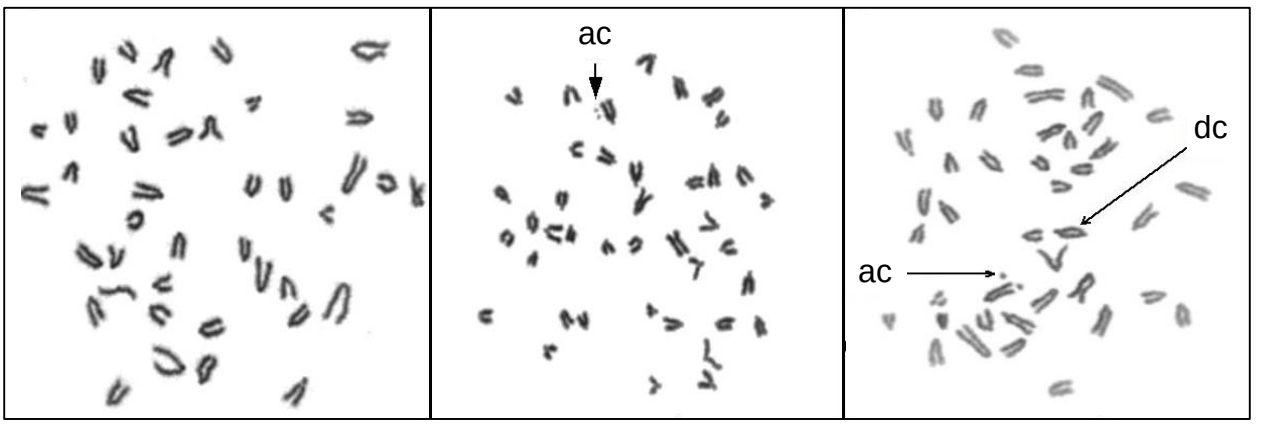
ac
dc
ac

Figure S1: Interaction between XRCC6 and RB1 in MCF-7 and HCT116 cells, Related to Figure 2

(A) RB1 immunofluorescence detection. MCF-7 cells transfected and treated in parallel and as for Figure 2D. The expression of RB1 was determined by immunofluorescence (red). Nuclei were visualised with Hoechst 33258.

(B) Proximity ligation probing for XRCC6/RB1 complex in HCT116 cells. Cells were subjected to treatment and processed as for Figure 2A. Signals pertinent to XRCC6/RB1 interactions are in red. Nuclei were visualised with Hoechst 33258. Scale bar represents 10 µm.

(C) Immunoblotting analysis of P-Ser780 RB1, serving as a biomarker for CDK4/6 activity. XRCC5 and XRCC6 total protein levels were also assessed. RB1 protein levels and tubulin levels are shown as loading controls. Cells were treated in parallel with, and as described for, samples analysed for Figure S1B.

(D) Proximity ligation probing for XRCC6/RB1 complexes in HCT116 cells treated with non-targeting (siNT) or RB1 targeting siRNA**.** Cells were treated and processed as for Figure 2D.

(E) RB1 Immunofluorescence detection. The expression of RB1 was determined by immunofluorescence (red). HCT116 cells transfected as in (D). Nuclei were visualised with Hoechst 33258. Scale bar represent 10 µm.

(F and G) Proximity ligation control reactions carried out in MCF-7 cells (F) and HCT116 cells (G). Either secondary probes alone (no Ab) were used, or secondary probes in combination with primary antibodies for XRCC6 or RB1 individually or in combination. Nuclei were visualised with Hoechst 33258. Samples were run in parallel with those shown in Figure 2A (MCF-7 cells) and Figure S1G (HCT116 cells). Scale bars show 10 µm.

Figure S2: Cell synchronisation and PLA staining, Related to Figure 2

(A) Workflow diagram for generation of cell cycle synchronised cell populations. MCF-7 and HCT116 were enriched for cells in G1, mid-S or G2/M phase of the cell cycle**.** S phase and G2/M enriched cell populations were generated using a double thymidine block (2 µM) followed by release into medium containing nocodazole (100 nM). Cells were harvested either 2 h (HCT116 mid-S phase enriched)/ 3 h (MCF-7 mid-S phase enriched) or 8 h later (HCT116 G2/M phase enriched)/ 10 h (MCF-7 G2/M phase enriched). Alternatively, cells seeded in parallel were exposed to 400 nM PD0332991 for 17 h (HCT116) or 19 h (MCF7).

(B) Cell cycle profiles of HCT116 subjected to procedures in (A), as determined by propidium iodide staining and flow cytometry. Error bars represent ± S.D for n = 3 biological replicates.

(C) Immunoblotting analysis depicting levels of RB1, XRCC5 and XRCC6 protein. Actin levels are shown as loading controls.

(D) Detection of RB1/XRCC6 complex in cell cycle phase enriched HCT116 cells. Complexes were detected using proximity ligation. Nuclei were visualised with Hoechst 33258.

(E) Automated quantification of foci number. Cumulative data for n=3 biological replicates are shown, representing quantification for a minimum of 100 independent cells. Quantification was performed as for Figure 2B, F.

Figure S3: Interaction of NHEJ component XRCC6 with RB family proteins, Related to Figure 3

(A) RB family protein sequence alignment. Sequences represent GST fusion proteins used in (B). The Alignments were generated using MultAlin V5, with hierarchical clustering for maximal amino acid similarity. Consensus levels: red = 100 % blue = 66 %. Consensus symbols: ! Either Ile or Val ; $ either Leu or Met; % either Phe or Tyr; # any of Asn, Asp, Gln or Gl. The position of sequence alterations (240-242 deletion and PolyG) associated with loss of interaction between RB1 to XRCC6 indicated by green coloured overly. The position of the cyclin fold helixes a1-a5 generating cyclin fold (CF) scaffolds A and CF scaffold B in RB1 N are indicated. CF A; cyclin fold A, CF B; cyclin fold B.

(B) Affinity enrichment analysis. Experiments were done using conditions as in Figure 1B-G. Purified recombinant RB family proteins N domain fragments (RB1 (aa 40-355), RBL1 (aa 19-330), RBL2 (aa 24-418) were expressed fused to GST and purified. Fusion proteins bound to Glutathione-resin were incubated with chromatin extract from 1 x 10^6 HCT116 cells as for Figure 1. Bound material was assessed for the presence of the NHEJ component XRCC5. GST alone was used as a negative control.

Figure S4: A role for $RB1^N$ in NHEJ, Related to Figure 4

(A) NHEJ proficiency in SAOS-2 cells transfected with empty vector or vector expressing RB1 or $RB1^{240\text{-}242\text{deletion}}$ variant. Data evaluation was as for Figure 4. Values for cells transfected with empty vector were set to 1.

(B) Cell cycle profiles of reporter transfected SAOS-2 cells, analysed as for Figure 4B. Profiles with a secondary nocodazole block are shown. Data represent transfected cell fractions deduced using DsRed for gating.

(C) Immunodetection of RB1 and $RB1^{240-242}$ in SAOS-2 cells from (A), loading was normalised for co-transfected DsRed expression plasmid.

(D) Proficiency of 240-242 to inhibit cell cycle progression in SAOS-2. Graph depicts stable G1 arrest, assessed by propidium iodide flow cytometry in cells with secondary nocodazole block. SAOS-2 cells transfected with empty vector, RB1 or 240-242 expression vectors.

(E) Proficiency of $RB1^{240-242}$ to inhibit colony formation. SAOS-2 transfected with empty vector, RB1 or 240-242 expression vector in combination with vector for puromycin resistance and scored for outgrowth of puromycin resistant colonies. Co-transfected β-galactosidase was used to normalise data to transfection efficacy.

(F) Immunodetection of RB1 and $RB1^{240-242}$ in SAOS-2 used in (D and E), loading was normalised using co-transfected EGFP expression plasmid.

(G) Proficiency of $RB1^{240-242}$ to regulated E2F activity. E2F reporter activity in SAOS-2 cells. Cells were transfected with RB1 or 240-242 or empty expression vector together with E2F promoter luciferase reporter. Co-transfected β-galactosidase was used to normalise data to transfection efficacy.

(H) Immunodetection of RB1 and $RB1^{240-242}$ in SAOS-2 used in (G). Loading was normalized to β-galactosidase activity. For all experiments the average for n = 3 biological replicates is depicted, error bars ± S.D * $p<0.05$ ** $p<0.01$ ***$p<0.001$ using a paired Student's t-test.

Figure S5: DNA content profiles of MEFs over irradiation time course, Related to Figure 5

(A-E) Integrated Hoechst 33258 staining intensity histogram for the three MEF backgrounds at various time points post 5 Gy IR. Wild type, RB1-/- or RB1/RBL1/RBL2 null (TKO) mouse embryonic fibroblasts (MEFs) were exposed to 5 Gy IR and stained for γH2AX and

DNA (using Hoechst 33258). Hoechst 33258 staining intensity (integrated mean) was determined for all cells from 30 independent eye fields and the distributions from one representative experiment are shown (A-E).

(F-J) Percentage of cells with < 2n, 2n, 4n and > 4n DNA content determined by gating (dotted line). Error bars represent ± S.D for n = 3 biological replicates.

Figure S6: Effect of RB family loss on DSB repair, Related to Figure 6

(A) Single cell comet analysis. HCT116 with and without siRNA-mediated ablation of RB family proteins (left) and congenic normal MEFs (wt) and MEFs with RB family gene deletion (TKO). Representative raw images are shown. Data relate to Figure 6A.

(B) Chromosomal aberration analysis in MEFs. Data for normal MEFs (wt) and MEFs with RB family gene deletion (TKO) are shown. Bars represent the frequency of cytogenetic aberrations detected per cell, considering both chromosome and chromatid aberrations. For each condition n = 50 metaphases were scored. Error bars represent SEM. For raw numerical scores see Table S4.

(C) Examples of Giemsa-stained MEF metaphases used for chromosome aberration analysis shown in B. Aberrations denoted by arrows, dicentrics (dc), excess acentric (ac).

Name	Uniprot Accession	Scaffold Probability	Mascot Score	Unique Peptides	Sequence Coverage (%)
DNA-dependent protein kinase catalytic subunit (PRKDC)	P78527	99.97	2299.7	13.33	47
Very long-chain specific acyl-CoA dehydrogenase (ACADV)	P49748	100	2016	49	27
ATP-dependent DNA helicase 2 subunit 2 (XRCC5)	P13010	100	1420.3	45.4	27.33
ATP-dependent DNA helicase 2 subunit 1 (XRCC6)	P12956	100	1174.7	40	23.33
Lamin-A/C (LMNA)	P02545	100	515.3	26	16
Poly [ADP-ribose] polymerase 1 (PARP1)	P09874	100	494	17.2	13.7
60 kDa heat shock protein (CH60)	P10809	100	435	26	11.33
Heterogeneous nuclear ribonucleoprotein M (HNRPM)	P52272	100	332.7	12.57	8.33
Histone H1.2 (H12)	P16403	99.93	275.3	19.13	5.67
Probable ATP-dependent RNA helicase DDX5 (DDX5)	P17844	100	246	9.5	6.37
TAR DNA-binding protein (TADBP)	Q13148	99.93	156.3	8.6	3
Histone H1.5 (H15)	P16401	100	150.7	13	3.33
DNA ligase 3 (DNLI3)	P49916	100	107.3	4.37	3.67
Nucleolar RNA helicase 2 (DDX21)	Q9NR30	100	100.7	5.27	2.67
Synaptic vesicle membrane protein VAT-1 homolog (VAT1)	Q99536	99.93	98.3	7.83	2.33
Carbamoyl-phosphate synthase (CPSM)	P31327	100	95	2.27	3.33
Serine hydroxymethyltransferase (GLYM)	P34897	100	91.3	10.3	4
Heterogeneous nuclear ribonucleoprotein A1 (ROA1)	P09651	99.7	81.7	7.13	1.67
Tubulin alpha-1A chain (TBA1A)	Q71U36	99	81	7.17	2.33
Ribonucleoprotein PTB-binding 1 (RAVR1)	Q8IY67	99.9	79.7	5.7	2.33
Bifunctional methylenetetrahydrofolate dehydrogenase (MTDC)	P13995	99.8	76.3	7.5	1
Serine/threonine-protein kinase PLK1 (PLK1)	P53350	99.5	76.3	3	1.67
Elongation factor Tu (EFTU)	P49411	99.85	71.3	3.6	1.3
Mitochondrial ribonuclease P protein 1 (MRRP1)	Q7L0Y3	100	65.7	4.23	1.67
Medium-chain specific acyl-CoA dehydrogenase (ACADM)	P11310	99.85	63.7	3.57	1.33
Matrin-3 (MATR3)	P43243	100	58.7	2.5	1.67
Tubulin beta chain (TBB5)	P07437	99.5	58.7	3.9	1.33
T-complex protein 1 subunit gamma (TCPG)	P49368	99	57.3	2.57	1.33
ATP-dependent RNA helicase DDX39 (DDX39)	O00148	100	57	3.6	1.33
L-lactate dehydrogenase A chain (LDHA)	P00338	99	56.7	3.2	1
Signal recognition particle 72 kDa protein (SRP72)	O76094	99.4	51	2.23	1
Histone-binding protein RBBP7 (RBBP7)	Q16576	99.9	50.7	2.43	1
Nucleophosmin (NPM)	P06748	100	45.3	9.83	1.3
Ras GTPase-activating-like protein (IQGA1)	P46940	99.8	42.3	0.87	1.33

Table S1. Table of $RB1^N$ interactors, Related to Figure 1. Table S1 lists candidate proteins found to interact with $RB1^N$ in two or more repeat pulldown reactions, ranked by their average Mascot score. The average probability as determined by Scaffold 3, the percent average sequence coverage and average number of unique peptides for each candidate protein is shown.

Condition A	Condition B	P value
Untreated	PD0339921 treatment	0.005
Untreated	5 Gy IR	<0.0001
Untreated	5 Gy IR plus PD0339921 treatment	<0.0001
PD0339921 treatment	5 Gy IR	0.211464
PD0339921 treatment	5 Gy IR plus PD0339921 treatment	<0.0001
5 Gy IR	5 Gy IR plus PD0339921 treatment	<0.0001

Table S2. Statistical test results for PLA detecting the interaction between RB1 and XRCC6 in MCF-7 cells, Related to Figure 2. Table S2 lists p-values from pair-wise comparison of population data depicted in Figure 2B, as determined by the Mann Whitney U test.

Condition A	Condition B	MCF-7 cells P value	HCT116 cells P value
G1 enriched	S phase enriched	<0.001	<0.001
G1 enriched	G2/M phase enriched	<0.001	<0.001
S phase enriched	G2/M phase enriched	0.0104	0.2454

Table S3. Statistical test results for PLA detecting the interaction between RB1 and XRCC6 in cell cycle phase enriched MCF7 and HCT116 populations, Related to Figure 2. Table S3 lists p-values from pair-wise comparison of population data depicted in Figure 2F and Figure S2E, as determined by the Mann Whitney U test.

Cells	Dose (Gy)	Total cells scored	Normal	Chromosome aberrations				Chromatid aberration					Mitotic Index
				Dicentrics	Dentric rings	Excess acentics	Total chromosomal	Chromatid gaps	Chromatid breaks	Iso chromatid gaps	Chromatid exchanges	Total chromatid	
MEFs Wild- type	0	**50**	49	0	0	0	**0**	0	1	0	0	**1**	3.2
	1	**50**	38	4	0	5	**9**	1	2	0	0	**3**	0.6
	2.5	**50**	26	3	0	29	**33**	3	2	0	0	**4**	0.4
MEFs TKO	0	**50**	49	0	0	0	**0**	0	2	0	0	**2**	4.6
	1	**50**	38	2	1	12	**14**	2	1	0	0	**4**	4.8
	2.5	**50**	27	6	0	33	**39**	1	1	0	1	**3**	1.8
HCT116 NT	0	**50**	41	0	0	1	**1**	1	7	0	0	**8**	28.0
	1	**50**	28	6	0	15	**21**	5	7	0	0	**12**	22.0
	2.5	**50**	18	25	0	37	**62**	3	3	1	0	**7**	11.4
HCT116 MOCK	0	**50**	46	0	0	0	**0**	1	2	1	0	**4**	26.2
	1	**50**	32	5	0	13	**18**	3	2	0	0	**5**	21.7
	2.5	**50**	14	15	0	25	**40**	3	7	1	1	**12**	15.1
HCT116 LIG4	0	**50**	45	0	0	0	**0**	1	3	0	0	**4**	29.9
	1	**50**	27	7	0	12	**19**	5	8	0	0	**13**	21.5
	2.5	**50**	11	19	0	43	**62**	4	10	0	2	**16**	9.1
HCT116 RB1,L1,L2	0	**50**	45	0	0	1	**1**	0	4	0	0	**4**	34.1
	1	**50**	29	2	0	14	**16**	6	16	0	0	**22**	31.6
	2.5	**50**	14	18	0	32	**50**	2	12	0	1	**15**	16.8

Table S4. Chromosomal radiation sensitivity data summary, Related to Figure 6. Table S4 summarises type and frequencies of chromosome and chromatid aberrations in first post-irradiation metaphases, related to supplemental Figure S6 (MEF data) and Figure 6 (HCT116 data).

SUPPLEMENTAL EXPERIMENTAL PROCEDURES

GST fusion protein purification. Rosetta^{TM} *E. coli* (Merck) were transformed with relevant GST constructs. Expression was induced with 200 μM IPTG (Sigma) at A600 = 0.6-0.7 at 20 °C for 18 h. Induced E. coli bacteria were sedimented by centrifugation and resuspended in extraction buffer (20 mM Tris-Cl pH 7.5, 80 mM NaCl, 5 mM DTT, 1 mM EDTA) with one complete protease inhibitor tablet (Roche). Suspensions were sonicated until the bacteria lysed, and cleared by centrifugation (20,000 g) for 1 h at 4 °C. For large scale preparations supernatants were purified using Q-Sepharose, followed by Glutathione Sepharose4 Fast Flow resin (GE Healthcare). Fusion proteins were bound to the resin in extraction buffer supplemented with 10 mM $MgCl_2$, 1 mM $MnCl_2$, 50 U/ml DNase I and 14 U/ml RNase A and eluted with reduced L-Glutathione (Sigma). Eluted preparations were dialysed into 20 mM Tris pH 7.5, 50 mM NaCl, 5 mM DTT and 1 mM EDTA. Protein concentrations were estimated by UV-Spectroscopy.

Mass spectrometry. GST affinity purified material was run into a 12 % Bis-Tris gel (Invitrogen), the protein containing region was excised as a single fraction, the gel slice was washed with 100 mM ammonium bicarbonate treated with 20 mM dithiothreitol (Sigma) (60 °C, for 1 h) followed by 60 mM Iodoacetamide (Sigma) (at room temperature in the dark for 45 min), then washed and dehydrated and incubated with 12.5 ng/ μl trypsin (Promega, Grade IV) for 45 min. After the incubation the supernatant was replaced with 100 mM ammonium bicarbonate and the digestion was allowed to proceed overnight at 4 ºC. Gel samples were washed with acetonitrile and 100 mM ammonium bicarbonate, treated three times each and the supernatant containing the digested peptides was collected

after each wash. Supernatants containing the tryptic peptides were concentrated in a speed vacuum unit. Tryptic peptides were resuspended in 30 µl of 0.1 % acetic acid and loaded on a 10 cm (bed length) self-packed C18 (YMC-Waters 10 µm) capillary pre-column (360 µm o.d. x 100 µm i.d.). After a 10 min rinse with 0.1 % acetic acid, the pre-column was connected to a 10 cm (bed length) self-packed 5 µm C18 (YMC-Waters ODS- AQ) analytical capillary column (360 µm o.d. x 50 µm i.d.) with an integrated electrospray tip (less than 1 µm orifice). Peptides were eluted with a 120 min gradient with solvents A (1 % acetic acid in SQ water) and B (90 % MeCN in 1 % acetic acid in SQ water): 10 min from 0 % to 15 % and 110 min from 15 % to 100 %, then directly electrosprayed into a quadrupole time of flight (QqTOF) mass spectrometer (QSTAR Elite, Applied Biosystems). The instrument was run in positive ion mode and MS/MS spectra of the five most intense peaks (exceeding 50-70 counts) with two to five positive charge states in the full MS scan were automatically acquired in information-dependent acquisition, target ions were excluded from further fragmentation for 50 to 60 seconds. The MS/MS accumulation was automatic, the fragment intensity multiplier set between 6 and 7 and the maximum accumulation was 3 seconds. MS/MS spectra were extracted and searched using Mascot version 2.1 (Matrix Science). Data was searched against the Swissprot human non- redundant protein database with trypsin specificity, allowing a maximum of two missed cleavages, with set mass tolerance of 2.2 Da for the precursor ion and 0.15 Da for the fragment ion. Data was search with fixed modification of carbamidomethyl (C) and variable modification of oxidation (M).

Mass spectrometry data analysis. Raw mass spec data were analysed using Mascot version 2.1 (Matrix Science, (http://www.matrixscience.com) followed by Scaffold 3 (Proteome Software). In order to be considered as hit, proteins had to score with a probability assigned by Scaffold of greater than 95 % and have at least two peptides identified that were

assigned greater than 90 % probability of being correctly identified from the spectra. Protein lists identified in GST and GST-$RB1^N$ sample were compiled and proteins that qualified as hits in corresponding GST preparations were eliminated from the corresponding $RB1^N$ list. In order to generate a consolidated list of candidate binding proteins, the candidate proteins had to be present in two or more independent $RB1^N$ replicate runs. To further confirm the identity of peptides, manual sequencing the fragmentation spectra for selected candidates were performed.

Gene ontology analysis. DAVID functional annotation tool (http://david.abcc.ncifcrf.gov, Dennis et al., 2003) was used to identify gene ontologies enriched over a self-generated nuclear protein background database. To generate the background list, the entire proteome (obtained from Swissprot) was uploaded as a list to DAVID using Uniprot Accession Numbers and proteins classified as nuclear using GOTERM_CC_FAT were collated. The list of interacting proteins was uploaded to DAVID using Swissprot identifiers and compared to this background using GOTERM_BP_FAT. Gene ontologies that show ten-fold or greater enrichment over backgrounds and contained three or more protein hits were considered enriched.

Mammalian cell extract preparation. Cell nuclear extracts were prepared for GST affinity purification experiments. MCF-7 and HCT116 nuclear extract was generated from log phase cells. Cell monolayers were washed with PBS and nuclei generated by re-suspending them into 10 mM Tris pH 7.5, 10 mM KCl, 1.5 mM $MgCl_2$, 0.1 mM TCEP and 0.5 % Triton (1×10^6 cells in 100 µl, at 4 °C). Suspensions were gently homogenized using a loose fitting pestel and nuclei sedimented (10,000 g for 20 min). HeLa nuclei (Cilibiotech) were

purchased from Cilibiotech. For extraction, nuclei were resuspended in three volumes of 30 mM Tris pH 7.5, 2.5 % Glycerol, 0.4 M NaCl, 1 mM $MnCl_2$, 2 mM TCEP, 2 mM Na_3VO_4, 10 mM NaF, containing DNase 1 (50 U/ ml) and RNase A (14 U/ ml) with 1 complete protease tablet (Roche) per 50 ml, and homogenised using a loose fitting pestle. After 20 min incubation on ice, the debris was sedimented by centrifugation at 20,000 g for 30 min at 4 ºC and supernatants decanted. For large scale purifications nuclear supernatants were dialysed against binding buffer (30 mM Tris pH 7.5, 2.5 % Glycerol, 80 mM NaCl, 0.1 mM EDTA, 0.1 mM TCEP). Any precipitates were removed by centrifugation (20,000 g for 1 h). Extracts were precleared by incubation with Glutathione Sepharose 4 Fast Flow bound GST (2 mg of GST for 2.5 x 10^9 nuclei) overnight at 4 ºC. The resin-bound GST was removed by centrifugation (1000 g for 5 min) and the supernatant collected. Protein concentrations in precleared lysates were estimated by DC Protein Assay (Bio-Rad). For small-scale affinity purification nuclear extracts were diluted three fold in binding buffer. To generate total cell lysates for immunoblotting cell monolayers were washed with PBS followed by extraction buffer (50 mM Tris pH 7.4, 250 mM NaCl, 1 mM DTT, 1 mM EDTA, 1 mM NaF, 10 mM β-glycerophosphate, 0.1 mM $NaVO_4$ plus Roche complete proteinase inhibitors) without Triton-100, then scraped into extraction buffer containing 0.2 % Triton X-100, and incubated on ice for 10 min. Extracts for the analysis of NHEJ components were generated by adding SDS loading buffer directly to these lysates. Lysates were spun though glass wool plugs to remove nucleic acid. For immunodetection of RB1, lysates were centrifuged at 10,000 g for 20 min to remove insoluble material.

GST affinity purification. Large-scale purifications used 2 mg of purified GST RB^N or GST protein bound to 200 µl Glutathione Sepharose 4 Fast Flow resin which was incubated with 0.7 mg pre-cleared HeLa nuclear extract for 2 h with 4 ^{0}C. Following incubation resins were

washed three times with binding buffer (30 mM Tris pH 7.5, 2.5 % Glycerol, 80 mM NaCl, 0.1 mM EDTA, 0.1 mM TCEP) and once with binding buffer containing 150 mM NaCl. Associated proteins were eluted with binding buffer containing 1 M NaCl. Affinity purified materials were fractionated on a 12 % Bis-Tris gel (Invitrogen). For small scale affinity purification 400 µl of MCF-7 or HCT116 extract was incubated with 400 µg Glutathione Sepharose 4 Fast Flow bound GST-RB^N or GST and bound to for 2 h at 4 °C. Associated proteins were eluted with 4 x SDS protein loading buffer and analysed by immunoblotting.

Co-immunoprecipitation. Cell nuclei were prepared as for GST affinity purification. Nuclear proteins were extracted in 0.32 M sucrose, 50 mM Tris (pH 7.5), 4 mM $MgCl_2$, 1 mM $CaCl_2$, 0.1 mM AEBSF containing 10 U per 2 x 10^6 cells micrococcal nuclease (New England Biolabs), with digestion for three hours at room temperature, supernatants were collected and residual soluble material extracted from the insoluble fraction using 1 mM Tris-HCl (pH 7.4), 10 mM EDTA, 1 mM AEBSF, 0.32 mM sucrose and 150 mM NaCl. RB1 was immunoprecipitated from this extract using rabbit serum against a human RB1 C-terminal fragment (aa 763-928) (Zarkowska and Mittnacht, 1997) crosslinked Protein A/G Plus^{TM} Agarose (Thermo Fisher). Immunoprecipitates were washed and precipitated proteins eluted according to the manufacturer's instructions. Eluted proteins were subjected to immunoblotting.

Proximity ligation assay. Proximity ligation assays were performed using Duolink technology (Cambridge Biosciences) in accordance with the manufacturer's recommendations. Cells were grown on eight well µ-slides imaging slides (Ibidi). Where

applicable cells were reverse transfected with siRNA using HiPerFect lipid transfection reagent (Qiagen) with a fixed siRNA concentration of 20 nM prior to seeding onto Ibidi µ-slides. Cells were exposed to 500 nM PD0332991 for 18 h where indicated and subjected to 5 Gy irradiation or mock irradiated where indicated. Cells were fixed with 4 % w/v formalin (Sigma) for 20 min at room temperature, reacted with mouse anti-RB1 (BD Pharmingen) in combination with goat anti-XRCC6 (raised in goat, Santa Cruz), all at a dilution of 1:250, overnight at 4 °C. Proximity of primary antibody reactivity was detected by PLA probes (MINUS Goat and PLUS Mouse) followed by a ligation and amplification reaction as described in the manufacturer's instructions. Slides were imaged using a Nixon Confocal microscope. Controls were carried out to ensure the signals were protein and interaction selective. The Cell profiler was used for signal quantification using the example speckle counting pipeline. For immunofluorescence staining parallel specimen were permeabilised with 1 % Triton X-100 in Tris buffered salt (TBS) and blocked with blocking buffer (5 % Milk powder in TBS with 1 % Tween). Immunostaining was performed as for the detection of γH2AX.

Cells, cell culture and cell synchronisation. HeLa cell nuclei were purchases from CIL BIOTECH s.a. HCT116, MCF-7, U2OS, SAOS-2 cells were purchased from American Type Culture Collection (ATCC). Wild type and congenic $RB1^{-/-}$ primary mouse embryonic fibroblasts (MEFs) were derived from individual day 13.5 embryos as previously described (Alani et al., 2001). TKO MEFs were provided by Professor H Te Riele, Netherlands Cancer Institute (Dannenberg et al., 2000). All MEFs had 129/Ola background. The CDK4/6 selective inhibitor PD0332991 (Fry et al., 2004) was obtained from Axon. In order to study cell cycle checkpoint regulation, nocodazole was used to induce a cell cycle

arrest in transfected TKO MEFs. Cells were treated with 0.5 µg/ml nocodazole (Sigma, www.sigmaalrich.com) for 24 h prior to harvest. NU7441 (Tocris) was used as an inhibitor of PRKDC, a protein required for classic NHEJ (Zhao et al., 2006). Cells were treated with 5 µM NU7441 24 h prior to 5 Gy irradiation or for the duration of the NHEJ reporter assay. MCF-7 and HCT116 cells were synchronised in the G1, S or G2/M phases of the cell cycle. G1 enriched HCT116 and MCF7 cells were generated by treatment with 400 nM PD 033299 for 17 h (HCT116) or 19 h (MCF-7). S phase and G2/M cells underwent a double thymidine block (2 µM) followed by release into nocodazole (100 nM). MCF-7 cells were harvested 3 h (S phase enriched) or 10 h later (G2/M phase enriched). HCT116 cells were harvested 2 h (S phase enriched) or 8 h (G2/M phase enriched) after release into nocodazole. Cell cycle distributions were assessed using propidium iodide staining and flow cytometry. Ser780 phosphorylation on RB1, representing as surrogate biomarker for active CDK4/6 was assessed using immunoblotting. DNAPK inhibitor Nu7026 was used at a final concentration of 10 µM. Inhibitors were added 1 h prior to irradiation and remained present throughout the remainder of the experiment.

Cell irradiation. Irradiation of cells was performed using an AGO HS 320/260 electrical source Xray set, with a dose rate of 5 Gy/min. Irradiation was conducted at room temperature except for Comet analysis where cells were placed on ice prior to irradiation. Following irradiation cells were immediately returned to a humidified incubator at 37 ^{0}C with 5 % CO_2.

Analysis of Chromosomal radiosensitivity. Cells were plated in 6-well dishes such that they were no more than 50 % confluent at the time of harvest. Cells transfected with siRNA were used 48 h post-transfection. Cells were detached using warm trypsin solution, trypsin

was neutralised with an equal volume warm culture medium and cells sedimented by centrifugation at 800 rpm for 5 mins. The supernatants were removed and cells resuspended in 1 ml of warm medium. 5 ml of warm 0.4 % KCl were added and cells incubated for 15- 30 min at 37 ^{0}C. Three drops of fixative solution [methanol-acetic acid (3:1)] were added and cells were sedimented at 800 g for 8 min. The supernatant was removed and 5 ml of fixative was added drop-wise. Centrifugation and fixative addition was repeated two more times. Fixed cells were stored at -20 ^{0}C until analysis. Chromosome-type (dicentrics, centric rings and excess acentric fragments, i.e. those not associated with dicentrics) and chromatid-type aberrations (chromatid gaps, breaks and exchanges) were scored by eye at 1000x magnification under oil immersion using the Metafer® metaphase finding system (Zeiss, UK).

Comet analysis. Cells were plated in 6-well plates (1 x 10^5 cells/well). Wherever required cells were transfected with siRNA for 48 h prior to irradiation. At the time required irradiated cells were harvested using trypsin, resuspended in fetal calf serum containing 10 % DMSO and stored at -80 ^{0}C until analysis. COMET single cell gel electrophoresis (comet) assay was performed as described in (Spanswick et al., 2010). Immediately before analysis cells were thawed on ice and diluted in cold serum-free DMEM to give a final concentration of 2.5 x 10^4 cells/ml. All procedures were carried out in subdued lighting. 0.5 ml of the appropriate cell suspension (i.e. 1.25 x 10^4 cells) was mixed with 1 ml of melted 1 % low gelling temperature (LGT)-agarose in water then placed onto the centre of a microscopic slide pre-coated with 1 % type 1-A agarose in water. Duplicate replicates were generated for each condition. Cells were lysed by immersion of the slides for 1 h in alkaline lysis buffer (100 mM disodium EDTA, 2.5 M NaCl, 10 mM Tris–HCl pH 10.5) containing 1 % Triton X-100. Slides were washed every 15 min in distilled water for 1 h. Slides were then incubated in alkali buffer (50

mM NaOH, 1 mM disodium EDTA, pH 12.5) for 45 min followed by electrophoresis in the same buffer for 25 min at 18 V (0.6 V/cm), 250 mA. The slides were finally rinsed in neutralising buffer (0.5 M Tris–HCl, pH 7.5) and then saline. After drying, the slides were stained with propidium iodide (2.5 μg/mL) for 30 min then rinsed in distilled water. Images were visualised using a NIKON inverted microscope with high-pressure mercury light source, 510-560 nm excitation filter and 590 nm barrier filter at x20 magnification. Images were captured by an on-line CCD camera and analysed using Komet Analysis software 6.0 (Andor Technology, U.K.). For each duplicate slide 25 cells were analysed. The tail moment for each image was calculated as the product of the percentage DNA in the comet tail and the distance between the means of the head and tail distributions (Olive et al., 1990).

DNA Constructs. pGEX6p1 expressing human RB1 40-355, human RB1 40-355-$^{Poly\ G}$ and RB 40-355$^{240-242}$ are described in (Hassler et al., 2007). pGex6P1 expressing RBL1 19-330 and RBL2 24-418 were generated by cloning a PCR generated coding sequence in frame into the BamH1 site of pGEX6p1. NHEJ reporter plasmids pim-EJ5-GFP and pCBΔI-SceI are described in (Bennardo et al., 2008). pDsRed was obtained from Clontech. Plasmids pcDNA3 9E10 and pcDNA3 9E10 RB1, -3xWT-luc pCMV-E2F1 and pCMV-DP1 are described in (Chew et al., 1998), pcDNA3-9E10 RB1^{PolyG} and pcDNA3-9E10 RB1$^{240-242}$ was cloned by overlap extension polymerase chain reaction with primers: 5'-cgggatccatgccgcccaaaacc-3'; 5'-gacgagaggcaggtcctc-3'; and 5'-gaggacctgcctctcgtc-3'; 5'-gcggatccttatctctgtgtttcaaaactg-3' using pGEX6P1 RB1 40-355 ^{PolyG} or pGEX6P1 40-355 240-242 and pcDNA9E10 RB1 as templates, followed by insertion of the into pcDNA3-9E10 RB1 using BamHI and EcoRI sites.

Antibodies. Antibodies used for immunoblotting and immunostaining were mouse anti-XRCC5 (AB3107, Abcam), mouse anti-XRCC6 (MS-329, Thermo), mouse anti-RB1 (G3-245, BD biosciences), mouse anti-DsRed (E64-1077, BD biosciences), anti-RB1-PS780 rabbit monoclonal antibody (E182 , Epitomics), mouse anti-MYC tag (4A6, Upstate), rabbit anti-EGFP (26-39, Novagen), anti-mouse anti-alpha-tubulin (B-5-1-2, Invitrogen), anti-PRKDC-PS2056 (EPR5670, Abcam) and anti-PRKDC (3H6, Thermo). In house rabbit serum raised against a C-terminal human RB1 fragment (aa 763-928) was used for co-immunoprecipitation experiments. Rabbit anti-mouse IgG (M7023, Sigma) was used as an irrelevant control serum. Mouse anti-phospho γH2AX was purchased from Millipore (05-636), secondary antibodies 488 Alexa Fluor-conjugated anti-mouse IgG (A-110001, Invitrogen), 647 Alexa Fluor-conjugated anti-mouse IgG (A21236, Invitrogen) and 647 Alexa Fluor-conjugated anti-goat IgG (A21447, Invitrogen) were purchased from Invitrogen. Goat anti- XRCC6 (sc-1487, Santa Cruz) anti-RB1 (G3-245, BD biosciences) were used for PLA.

siRNAs and transfection. RB1 specific siRNA sequence GGUUCAACUACGCGUGUAAdTdT was from Dharmacon. RBL1 siRNA pool (M-003298-02, siGenome SMART pool) and RBL2 siRNA pool (M-003299-03, siGenome SMART pool) and LIG4 siRNA pool (M-004254-04, siGenome SMART pool) was purchased from Dharmacon. Non-targeting AllStars Negative Control siRNA, was obtained from Qiagen. siRNA transfections were performed using lipofectamine^{TM} (Life Technologies) according to the manufacturer's instructions using fixed total siRNA concentration of 20 nM.

Cell based assays for assessment of RB1 function. For G1 arrest assays SAOS-2 cells were electroporated with 0.2 µg pCMV-CD20, 1.6 µg pcDNA3-9E10 RB1 wild type or variant. Electroporation was carried out using Cell Line Nucleofector® Kit V (Lonza) according to manufacturer's instructions. Electroporated cells were seeded and 24 h later treated with 0.6 µg/ml nocodazole (Sigma) to distinguish cycling cells in G1 from cells arrested in G1. 24 h later non-adherent and adherent cells were collected in PBS/EDTA, washed with PBS, resuspended in PBS containing 5 µl FITC-conjugated anti-CD20 antibody (BD Pharmingen) and incubated at 4 °C for 30 min. Cells were washed with PBS and fixed in 70 % ethanol for 30 min at 4 °C. After fixation, PI stain was used to determine the percentage of cells in each cell cycle phase. To assess RB mediated reduction of colony outgrowth SAOS-2 cells were transfected with 1.6 µg pcDNA3-9E10 RB1 wild type or variant, 0.15 µg pBABE-puromycin, 0.1 µg RSV-β-galactosidase and 0.1 µg EGFP using electroporation as for G1 arrest analysis. 400 µl of the electroporated cell suspension was seeded into two 10 cm petri dishes in media containing 0.6 µg/ml puromycin to select for transfected cells. Colonies were counted after 14 days and normalised for β-galactosidase activity. The amount of colonies for the empty vector was set at 100 %. The remaining cells were grown for 36 h and harvested to quantify β-galactosidase activity and for monitoring RB1 transgene expression by immunoblotting. The GalactoLight β-Galactosidase Reporter Gene Assay System (Applied Biosystems) was used to quantify β-galactosidase activity, EGFP was immunoblotted alongside RB1 as an additional loading control. To assess E2F repression SAOS-2 cells were transfected with 0.1 µg pGL2-3xWT-luc, 0.01 µg pCMV-E2F1, 0.02 µg pCMV-DP1, 0.45 µg pcDNA3-9E10 RB1 wild type or variant, 0.1 µg RSV-β-galactosidase and 0.1 µg EGFP using electroporation as for G1 arrest analysis. The reporter construct contains an artificial promoter with three E2F binding sites connected to a luciferase reporter gene. Luciferase activity was determined after 40 h using the Luciferase Assay System (Promega) according to

manufacturer's instructions using a luminometer with an injector. Luciferase values were normalised to β-galactosidase activity.

REFERENCES

Alani, R.M., Young, A.Z., and Shifflett, C.B. (2001). Id1 regulation of cellular senescence through transcriptional repression of p16/Ink4a. Proceedings of the National Academy of Sciences of the United States of America *98*, 7812-7816.

Bennardo, N., Cheng, A., Huang, N., and Stark, J.M. (2008). Alternative-NHEJ is a mechanistically distinct pathway of mammalian chromosome break repair. PLoS genetics *4*, e1000110.

Chew, Y.P., Ellis, M., Wilkie, S., and Mittnacht, S. (1998). pRB phosphorylation mutants reveal role of pRB in regulating S phase completion by a mechanism independent of E2F. Oncogene *17*, 2177-2186.

Dannenberg, J.H., van Rossum, A., Schuijff, L., and te Riele, H. (2000). Ablation of the retinoblastoma gene family deregulates G(1) control causing immortalization and increased cell turnover under growth-restricting conditions. Genes & development *14*, 3051-3064.

Fry, D.W., Harvey, P.J., Keller, P.R., Elliott, W.L., Meade, M., Trachet, E., Albassam, M., Zheng, X., Leopold, W.R., Pryer, N.K., *et al.* (2004). Specific inhibition of cyclin-dependent kinase 4/6 by PD 0332991 and associated antitumor activity in human tumor xenografts. Molecular cancer therapeutics *3*, 1427-1438.

Hassler, M., Singh, S., Yue, W.W., Luczynski, M., Lakbir, R., Sanchez-Sanchez, F., Bader, T., Pearl, L.H., and Mittnacht, S. (2007). Crystal structure of the retinoblastoma protein N domain provides insight into tumor suppression, ligand interaction, and holoprotein architecture. Molecular cell *28*, 371-385.

Olive, P.L., Banath, J.P., and Durand, R.E. (1990). Heterogeneity in radiation-induced DNA damage and repair in tumor and normal cells measured using the "comet" assay. Radiation research *122*, 86-94.

Spanswick, V.J., Hartley, J.M., and Hartley, J.A. (2010). Measurement of DNA interstrand crosslinking in individual cells using the Single Cell Gel Electrophoresis (Comet) assay. Methods in molecular biology *613*, 267-282.

Zarkowska, T., and Mittnacht, S. (1997). Differential phosphorylation of the retinoblastoma protein by G1/S cyclin-dependent kinases. J Biol Chem *272*, 12738-12746.

Zhao, Y., Thomas, H.D., Batey, M.A., Cowell, I.G., Richardson, C.J., Griffin, R.J., Calvert, A.H., Newell, D.R., Smith, G.C., and Curtin, N.J. (2006). Preclinical evaluation of a potent novel DNA-dependent protein kinase inhibitor NU7441. Cancer research *66*, 5354-5362.